

THE 4TH INTERNATIONAL CONFERENCE ON ALUMINUM ALLOYS

EFFECT OF Ce ADDITION ON CORROSION BEHAVIOR OF Al-Li ALLOY 1430

Y. L. Wu¹, J. Qiang¹, Y. W. Li¹, Z. Lu¹, R. G. Ouyang¹, B. C. Liu¹,
N. I. Kolobnev², L. B. Khokhlatova²

1. Institute of Aeronautical Materials, Beijing

P. O. Box 81-2, Beijing 100095, P. R. China

2. All-Russian Institute of Aviation Materials, Moscow, Russian

Abstract

The effects of Ce addition on corrosion behavior of 1430 Al-Li alloy are discussed. The tests of intergranular attack, C-ring stress corrosion and oxidation resistance are carried out, the grain boundary structure is also studied by the TEM, SEM and EDAX. With addition of Ce, the precipitates in large-angle grain boundary are coarsened, which improves the corrosion resistance of 1430 alloy by slowing the anodic dissolution along grain boundary. It is also found that, 1430+Ce alloy could form more compact layer on its surface after oxidation than 1430 alloy, and this results in the oxidation resistance improvement obviously.

Key Words cerium, corrosion, Al-Li alloy 1430

Introduction

The Al-Li alloy 1430 is developed by All-Russian Institute of Aviation Materials (VIAM) in order to match the properties of conventional damage tolerant Al alloys such as 2024-T3. This alloy offers higher ductility ($\geq 10\%$), and also has about 8% density reduction and 10% modulus increasing when compared to 2XXX alloys. However, it exhibits poor corrosion resistance. Some research works have been carrying out on this problem by BIAM (Institute of Aeronautical Materials, Beijing) together with VIAM. The purpose of the present investigation is to improve the corrosion behavior by Ce addition in 1430 alloy. The corrosion phenomena like stress corrosion cracking (SCC) and intergranular attack are in the centre of interest.

Experimental Procedures

The chemical compositions of the 1430 alloys tested were shown in Table 1.

Table 1. Composition of Alloys (wt%)

Alloy	Li	Cu	Mg	Zr	Ti	Ce	Fe	Si
A	1.80	2.96	1.60	0.10	0.03	—	<0.05	<0.05
B	1.79	2.93	1.61	0.12	0.03	0.04	<0.05	<0.05

The ingots were semicontinuously direct chill cast in BIAM. After proper homogenization, the ingots were extruded to 11×55 mm shapes and $\phi 25$ mm bars. Both A and B alloy were heat treated to T6 condition.

Intergranular attack and SCC tests were carried out according to the GB7998-87 (aqueous NaCl+H₂O₂ solution) and HB5259-83 (aqueous 3.5% NaCl solution) respectively. The corrosion potential and current were determined by the Model 378 electrochemistry corrosion system (aqueous 3.5% NaCl solution, lab air, 35°C, potential scanning rate=0.5mv/sec). PE/DSC-2C was used to test the oxidation weight gaining of alloy A and B. The atmosphere was lab nitrogen. The microstructures of alloy A and B were studied, using H-800 TEM, JSM-840 SEM and TN-5500 EDAX.

Results and Discussion

Forms of Ce in 1430 Alloy

There are three forms for rare-earth elements in aluminum alloys: solution in α (Al) matrix; segregation in phase-boundary and grain-boundary; solution in compounds or as component of compounds. As the content of Ce in alloy B is very less, it exists mainly in the first two forms.

Fig. 1a is the SEM photo of alloy B. The fracture surface shows intergranular and intragranular features. Ce segregates in grain boundary, thus, it could be only found some particles which contain Ce element on the grain boundary. This has been confirmed by EDAX (Fig. 1b). Fig. 1c, d show the fine structure of grain boundary precipitate (R phase) which contains Ce in alloy B and its EDAX curve. Generally speaking, the grain

boundary precipitates of 1430 alloy are all T_2 phase (Al_6CuLi_3), R phase (Al_5CuLi_3) is in the grain. But it is of interest to note that there are a few R phase precipitate in the grain boundary and all of them contain Ce element. This is maybe caused by the $T_2 \rightarrow R$ transformation[1] which has been accelerated by the existence of Ce. Further works have been carrying on.

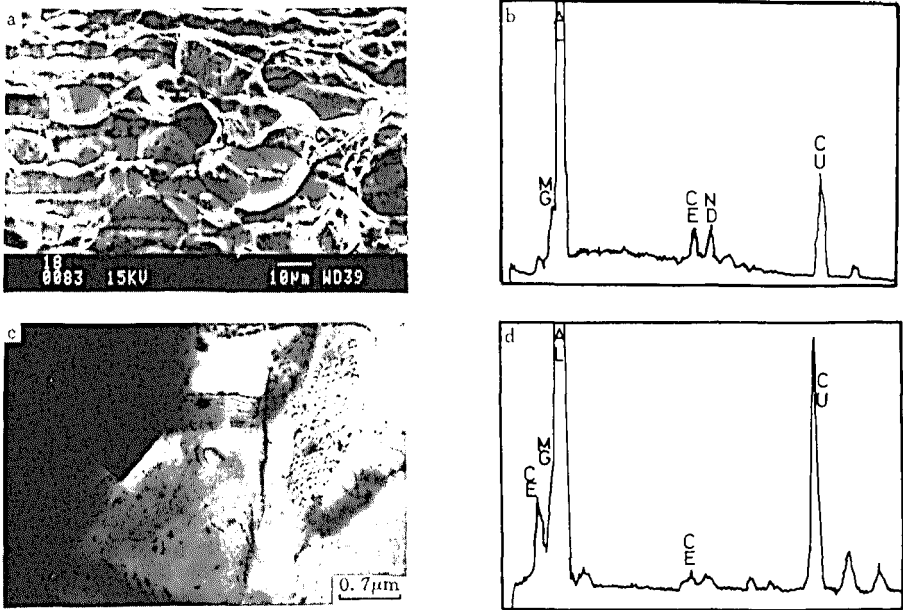


Figure 1. Morphology of Ce-contain particles in alloy B.

Intergranular Attack and SCC

The test results of intergranular attack ,SCC,corrosion current (I_{corr}) and corrosion potential (E_{corr}) are listed in Table 1 .

Alloy A and B have the similar intergranular attack feature, they also have the similar SCC feature except that the secondary cracking length of alloy A is longer than that of alloy B. After addition of Ce, the mean depth of intergranular attack decreases obviously (about 68%) and the mean time of SCC becomes longer (about 4~5 times). These results correspond to the change of corrosion current, that is, with the decreasing of corrosion current, the corrosion resistance enhances.

Table I. Results of Corrosion Tests

Alloy	Intergranular Attack		SCC	I_{corr}	E_{corr}
	Mean Depth (mm)	Grade	Mean Time (d)	($\mu\text{A}/\text{cm}^2$)	(v)
A	0.57	5	0.32/315MPa	4.23	-0.741
			0.55/270MPa		
			0.80/248MPa		
B	0.18	4	1.72/308MPa	2.57	-0.994
			2.48/264MPa		
			3.28/242MPa		

Corrosion potential of alloy B is more negative than that of alloy A, this means that alloy B has higher corrosion tendency in point of the thermodynamics. From polarizing curve (Fig. 2), it could be found that the anodic polarizing slope of alloy B is greater than that of alloy A. This indicates that alloy B has greater polarizing resistance (its anodic phase is passivated easily) which slows anodic dissolution rates. These could be referred to the change of grain boundary precipitates after Ce addition.

Figure 3 shows the fine grain boundary structures of alloy A (Fig. 3a) and B (Fig. 3b). A lot of grain boundary (GB) phases (T_2 phase mainly) precipitate in a row. As the GB precipitate is more anodic than the matrix[2], and thus, preferentially dissolves, so the GB precipitate which has small size and short distance would weaken the GB and cause the anodic dissolution easily. From Figure 3, it could be found that, with the addition of Ce, the size and distance of the GB precipitate increase. The larger GB phase could lead to crack blunting and the long distance may slow the crack growth. As to this, the anodic dissolution rate of alloy B is less than that of alloy A.

The corrosion behavior of precipitation-hardened alloys may depend on a large number of microstructural parameters that vary during fabrication and heat treatment, such as grain size, GB solute segregation, matrix precipitate size, GB precipitate size, PFZ size and matrix slip character. As there is no difference in these aspects except GB precipitate size of alloy A and B ($\sigma_{0.2}^A = 450\text{MPa}$, $\sigma_{0.2}^B = 440\text{MPa}$; $D_{Al_2Zr}^A \approx 7.5\text{nm}$, $D_{Al_2Zr}^B \approx 7.8\text{nm}$), the improve-

ment of SCC (and intergranular attack) of alloy B could be due to the increasing size of GB precipitate which is led by the addition of Ce.

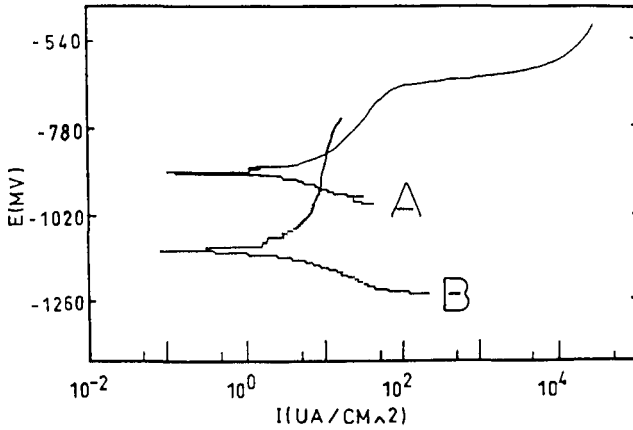


Figure 2. Polarizing curves of alloy A and B

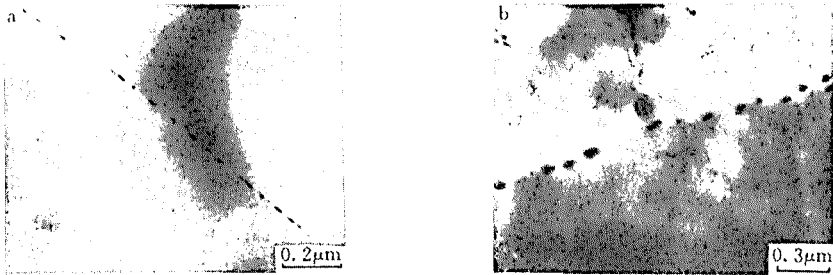


Figure 3. TEM photoes of alloy A and B

High Temperature Oxidation

Figure 4 shows the variation of weight-gaining ratio (per surface) vs temperature of al-

loy A and B in lab nitrogen. It could be found that alloy B has little weight-gaining in the range of ageing temperature ($<300^{\circ}\text{C}$). In the temperature range of hot work and solution ($300\sim 550^{\circ}\text{C}$), it also exhibits good oxidation resistance. In the whole temperature range of the test, alloy B has higher oxidation resistance than alloy A.

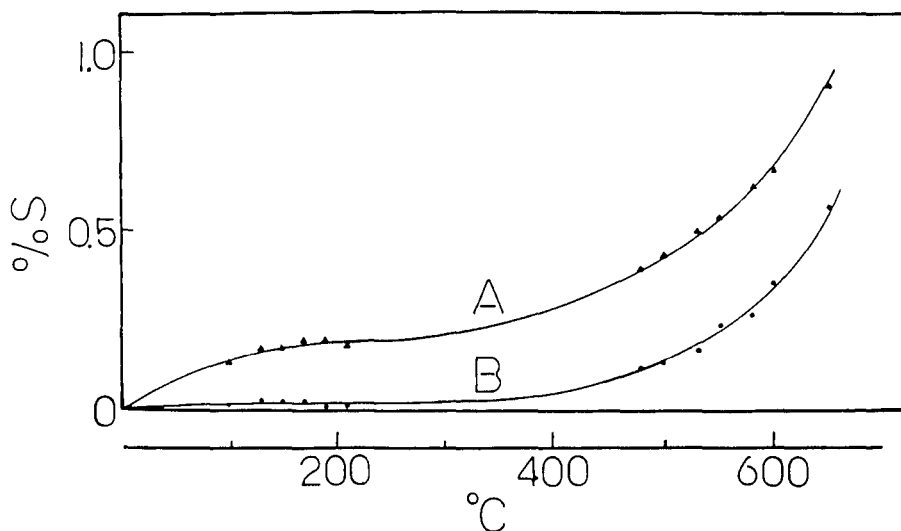


Figure 4. High temperature weight gaining curve of alloy A and B

From the $\Delta G^{\circ}-T$ equilibrium diagram of metal oxide, it could be seen that the standard generating free energy (ΔG°) of $4/3 \text{Ce} + \text{O}_2 \rightarrow 2/3 \text{Ce}_2\text{O}_3$ reaction is less than that of $4\text{Li} + \text{O}_2 \rightarrow 2\text{Li}_2\text{O}$ and $2\text{Mg} + \text{O}_2 \rightarrow 2\text{MgO}$ in the temperature range of $\text{RT} \sim 700^{\circ}\text{C}$. This means that Ce may have preferential oxidation tendency than Mg and Li. In addition, it could be found that the PB ratio (Pilling Bedworth ratio) of Ce_2O_3 film is greater than 1 ($\gamma_{\text{Ce}_2\text{O}_3} = 1.16$), the PB ratios of MgO and Li_2O film are all less than 1 ($\gamma_{\text{MgO}} = 0.99, \gamma_{\text{Li}_2\text{O}} = 0.57$) [3]. This indicates that the oxide film of Ce_2O_3 is compact, and that of Li_2O and MgO are porous which leads the water vapor penetrates easily and reacts continuously with the fresh metal. As to this, it could be concluded that the compact Ce_2O_3 film can increase

the oxidation resistance, and thus reduce the tendency of weight-gaining. This coincides with the work of Y. Zhang, et al [4].

Conclusions

1. There are two existential forms for trace element Ce in 1430 alloy: solution in α (Al) matrix and segregation in grain boundary precipitate. The addition of trace Ce has little effect on the strength, the precipitates in grain and so on.
2. The corrosion behavior of 1430 alloy has been improved by addition of Ce. This is due to that the growth of grain boundary precipitate has been accelerated by the Ce, and then the anodic dissolution is slowed.
3. Ce can oxide preferentially than Mg and Li, and the oxide film of Ce is compact, so the high temperature oxidation resistance of 1430 alloy is improved.

References

1. S. C. Wang, C. Z. Li and Y. L. Wu, J. Mater. Sci. Lett. 10, (1991), 643.
2. T. D. Burleigh, Corrosion 47, (1991), 89.
3. R. Z. Zhu, Metal Corrosion (Beijing, Metallurgical Industry Publishing House, 1989), 9.
4. Y. Zhang et al., 5th International Al-Li Conference, 1989, 539.